

Suspended graphene films and their Casimir interaction with ideal conductor

I. V. Fialkovsky *

*Instituto de Física, Universidade de São Paulo, São Paulo, S.P., Brazil
Department of Theoretical Physics, Saint-Petersburg State University, Russia*

We adopt the Dirac model for graphene and calculate the Casimir interaction energy between a plane suspended graphene sample and a parallel plane ideal conductor. We employ both the Quantum Field Theory (QFT) approach, and the Lifshitz formula generalizations. The first approach turns out to be the leading order in the coupling constant of the second one. The Casimir interaction for this system appears to be rather weak but experimentally measurable. It exhibits a strong dependence on the mass of the quasi-particles in graphene.

Present article is based on joint works.^{1,2}

Keywords: Casimir energy, graphene, QFT, Lifshitz formula

1. Introduction

Graphene is a (quasi) two dimensional hexagonal lattice of carbon atoms. It belongs to the most interesting materials in solid state physics now due to its exceptional properties and importance for nano technology.^{3,4} Here we consider the Casimir interaction between suspended graphene plane and parallel ideal conductor. This setup was considered in⁵⁻⁷ using a hydrodynamical model for the electrons in graphene following.^{8,9} Later it became clear that this model does not describe the electronic properties specific to this novel material.

Here we use a realistic and well-tested model where the quasi-particles in graphene are considered to be two-component Dirac fermions. This model incorporates the most essential and well-established properties of their dynamics: the symmetries of the hexagonal lattice, the linearity of the spectrum, a very small mass gap (if any), and a characteristic propagation velocity which is 1/300 of the speed of light.^{3,10} By construction, this model

*The author gladly acknowledge the financial support of FAPESP, as well as of grants RNP 2.1.1/1575 and RFBR 07-01-00692.

should work below the energy scale of about $1eV$, but even above this limit the optical properties of graphene are reproduced with a high precision.¹⁵

The action of the model, therefore, is given by

$$S_D = \int d^3x \bar{\psi}(\tilde{\gamma}^l(i\partial_l - eA_l) - m)\psi, \quad l = 0, 1, 2 \quad (1)$$

where $\tilde{\gamma}^l$ are just rescaled 2×2 gamma matrices, $\tilde{\gamma}^0 \equiv \gamma^0$, $\tilde{\gamma}^{1,2} \equiv v_F \gamma^{1,2}$, $\gamma_0^2 = -(\gamma^i)^2 = 1$. In our units, $\hbar = c = 1$, and Fermi velocity $v_F \simeq (300)^{-1}$. The value of the mass gap parameter m and mechanisms of its generation are under discussion.¹¹⁻¹⁴ The upper limit on m is about $0.1eV$ at most.

The propagation of photons in the ambient $3 + 1$ dimensional space is described by the Maxwell action

$$S_M = -\frac{1}{4} \int d^4x F_{\mu\nu} F^{\mu\nu}, \quad \mu, \nu = 0, 1, 2, 3. \quad (2)$$

In the following we shall suppose that the graphene sample occupies the plane $x^3 = a > 0$, and the conductor corresponds to $x^3 = 0$.

2. QFT approach

In the framework of QFT one evaluates the effective action in a theory described by the classical action $S_D + S_M$. Then the Casimir energy density per unit area of the surfaces at the leading order in the fine structure constant α is given by

$$\mathcal{E}_1 = -\frac{1}{TS} \text{Tr} \left(\text{Feynman diagram: a circle with a solid line and a wavy line} \right), \quad (3)$$

where T is time interval, and S is the area of the surface. The solid line denotes the fermion propagator in $2+1$ dimensions (i.e., inside the graphene sample), and the wavy line is the photon propagator in the ambient $3 + 1$ dimensional space subject to the perfect conductor boundary conditions at $x^3 = 0$: $A_0|_{x^3=0} = A_1|_{x^3=0} = A_2|_{x^3=0} = \partial_3 A_3|_{x^3=0} = 0$.

The fermion loop in $2 + 1$ dimensions has already been calculated in a number of papers.^{11,13,14} It gives the quadratic order in A of the effective action for electromagnetic field

$$S_{\text{eff}}(A) = A \text{Tr} \left(\text{Feynman diagram: a circle with a solid line and a wavy line} \right) A = \frac{1}{2} \int \frac{d^3p}{(2\pi)^3} A_j(p) \Pi^{jl}(p) A_l(p), \quad (4)$$

where

$$\Pi^{mn} = \frac{\alpha \Phi(\tilde{p})}{v_F^2} \eta_j^m \left(g^{jl} - \frac{\tilde{p}^j \tilde{p}^l}{\tilde{p}^2} \right) \eta_l^n, \quad (5)$$

is the polarization tensor in the lowest, one loop, order. Here $\eta_j^m = \text{diag}(1, v_F, v_F)$, \tilde{p} denotes the rescaled momenta $\tilde{p}_j = \eta_j^k p_k$. The function $\Phi(p)$ is model dependent, and for graphene it reads $\Phi(p) = 2(2m\tilde{p} - (\tilde{p}^2 + 4m^2)\text{arctanh}(\tilde{p}/2m)) / \tilde{p}$. We assume here that all possible parity-odd parts are canceled in Π . Possible effects invoked by their presence are considered in.¹

To calculate the diagram (3) we only need to couple the kernel (5) to the photon propagator subject to conducting boundary conditions. In Fourier representation and for the Euclidean 3-momenta, i.e., after the Wick rotation $p \rightarrow p_E = (ip_0, p_1, p_2)$, the a -dependent part of the energy reads

$$\mathcal{E}_1 = -\frac{1}{4} \int \frac{d^3 p_E}{(2\pi)^3} \frac{\Pi_j^j(p_E)}{p_{\parallel}} e^{-2ap_{\parallel}} = - \int \frac{d^3 p_E}{(2\pi)^3} \frac{\alpha(p_{\parallel}^2 + \tilde{p}_{\parallel}^2)\Phi(p_E)}{4p_{\parallel}\tilde{p}_{\parallel}^2} e^{-2ap_{\parallel}}. \quad (6)$$

where we expanded $\Pi_j^j(p_E)$ explicitly with help of (5), and $p_{\parallel} \equiv |p_E|$.

3. Lifshitz formula approach

One can also consider the system as described by effective theory of the electromagnetic field with the action $S_M + S_{\text{eff}}$ subject to the conducting boundary conditions at $x^3 = 0$. Then at the surface of graphene, the Maxwell equations receive a singular contribution

$$\partial_{\mu} F^{\mu\nu} + \delta(x^3 - a)\Pi^{\nu\rho} A_{\rho} = 0 \quad (7)$$

following from S_{eff} . Here we set $\Pi^{3\mu} = \Pi^{\mu 3} = 0$. This contribution is equivalent to imposing the matching conditions

$$(\partial_3 A_{\mu})|_{x^3=a+0} - (\partial_3 A_{\mu})|_{x^3=a-0} = \Pi_{\mu}^{\nu} A_{\nu}|_{x^3=a}. \quad (8)$$

assuming that A_{μ} is continuous at $x^3 = a$. Now, one can forget the origin of Π_{μ}^{ν} and quantize (at least formally) the electromagnetic field subject to the conditions (8) at $x^3 = a$ and to the conducting conditions at $x^3 = 0$.

The original Lifshitz approach¹⁷ was generalized^{18,19} for the interactions between two plane parallel interfaces separated by the distance a and possessing arbitrary reflection coefficients $r_{\text{TE},\text{TM}}^{(1)}$, $r_{\text{TE},\text{TM}}^{(2)}$ of the TE and TM electromagnetic modes on each of the surfaces

$$\mathcal{E}_L = \int \frac{d^3 p_E}{16\pi^3} \ln[(1 - e^{-2p_{\parallel}a} r_{\text{TE}}^{(1)} r_{\text{TE}}^{(2)})(1 - e^{-2p_{\parallel}a} r_{\text{TM}}^{(1)} r_{\text{TM}}^{(2)})]. \quad (9)$$

For graphene with help of matching conditions (8) we can obtain at the Euclidean momenta

$$r_{\text{TE}}^{(1)} = \frac{-\alpha\Phi}{2p_{\parallel} + \alpha\Phi}, \quad r_{\text{TM}}^{(1)} = \frac{\alpha p_{\parallel}\Phi}{2\tilde{p}_{\parallel}^2 + \alpha p_{\parallel}\Phi}, \quad (10)$$

while for the perfect conductor one has $r_{\text{TE}}^{(2)} = -1$, $r_{\text{TM}}^{(2)} = 1$. It is clear, that Φ must be rotated to Euclidean momenta as well. We also note that the perfect conductor case is recovered from (10) in the formal limit $\Phi \rightarrow \infty$.

One can show by a direct computation that the energy \mathcal{E}_1 , Eq. (6), coincides with the leading α^1 order in a perturbative expansion of the Lifshitz formula (9)-(10), so that the two approaches are consistent.

4. Results and discussion

The formulae (6) and (9)-(10) are suitable for the numerical and asymptotical evaluation. The asymptotic expansion for short and long distances are readily obtained through uniform expansion of the integrand of (6), (9)

$$\mathcal{E}_L \underset{a \rightarrow \infty}{\sim} -\frac{\alpha}{24\pi^2} \frac{2 + v_f^2}{ma^4}, \quad \mathcal{E}_L \underset{a \rightarrow 0}{\sim} \frac{1}{16\pi a^3} h(\alpha, v_F) \quad (11)$$

Note that the asymptotics at large separations is of the first order in α while for small separations, it contains all powers of α through $h(\alpha, v_F)$, for the real values of parameters in graphene $h(1/137, 1/300) \approx 0.024$.

Therefore we see that at large separations Casimir energy does not turn into the ideal conductor case, while at small separation this case is indeed recovered. This is counter-intuitive since the main contribution at short separations shall come from the high momenta for which one would expect the graphene film to become transparent. We must also stress that this behavior is drastically different from that in the hydrodynamic model.⁵⁻⁷

For numerical evaluation we normalize the results to the Casimir energy $\mathcal{E}_C = -\frac{\pi^2}{720a^3}$ for two plane ideal conductors separated by the same distance a . The results of calculations are depicted at Fig. 1. The scale is defined by the mass parameter m . For m of the order of next nearest-neighbor hopping energy t' , i.e., $m = 0.1eV$,⁴ $ma = 1$ corresponds to $a = 1.97$ micrometer.

Thus, we can see that the magnitude of the considered Casimir interaction of graphene with a perfect conductor is rather small. Actual measurement of such weak forces is a challenging, but by no means hopeless, experimental problem. Strong dependence on the mass parameter m at large separation is also a characteristic feature of the Casimir force. Getting an independent measurement of m may be very important for our understanding of the electronic properties of graphene. The mass of quasi-particles in graphene is, probably, very tiny, which improves the detectability of the Casimir interaction since the energy increases with decreasing m .

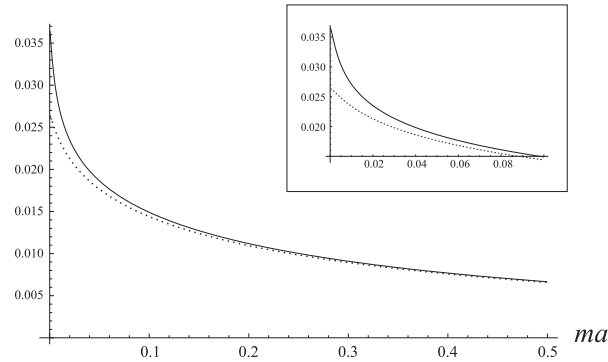


Fig. 1. The relative Casimir energy densities $\mathcal{E}_1/\mathcal{E}_C$ (solid line) and $\mathcal{E}_L/\mathcal{E}_C$ (dashed line) as functions of ma . Insert shows a zoom of the small-distances region.

References

1. I. V. Fialkovsky and D. V. Vassilevich, *J. Phys. A: Math. Theor.* **42** (2009) 442001 (6pp), arXiv:0902.2570 [hep-th].
2. M. Bordag, I. V. Fialkovsky, D. M. Gitman, D. V. Vassilevich, arXiv: 0907.3242 [hep-th]
3. A. K. Geim and K. S. Novoselov, *Nature Mater.* **6**, 183 (2007); M. I. Katsnelson, *Mater. Today* **10**, 20 (2007); A. K. Geim, arXiv:0906.3799.
4. A. H. Castro Neto, et al. *Rev. Mod. Phys.* **81**, 109 (2009).
5. G. Barton. *J. Phys.*, A38(13):2997–3019, 2005.
6. M. Bordag, *J. Phys. A* **39**, 6173 (2006) [arXiv:hep-th/0511269].
7. M. Bordag, et al. *Phys. Rev. B* **74**, 205431 (2006).
8. A. L. Fetter. *Annals of Physics*, **81**, 367, (1973).
9. G. Barton. *J. Phys. A: Math. Gen.*, **37**, 1011, (2004).
10. G. W. Semenoff, *Phys. Rev. Lett.* **53**, 2449 (1984); D. P. DiVincenzo and E. J. Mele, *Phys. Rev. B* **29**, 1685 (1984);
11. T. W. Appelquist, et al. *Phys. Rev. D* **33**, 3704 (1986).
12. D. V. Khveshchenko, *Phys. Rev. Lett.* **87**, 206401 (2001).
13. E. V. Gorbar, et al., *Phys. Rev. B* **66**, 045108 (2002), V. P. Gusynin and S. G. Sharapov, *Phys. Rev. B* **73**, 245411 (2006)
14. P. K. Pyatkovskiy, *J. Phys.: Condens. Matter* **21**, 025506 (2009).
15. R. Nair, et al. *Science* **320**, 1308 (2008).
16. M. Bordag, I. G. Pirozhenko and V. V. Nesterenko, *J. Phys. A* **38**, 11027 (2005) [arXiv:hep-th/0508198]; D. V. Vassilevich, *Phys. Rev. D* **79**, 065016 (2009) [arXiv:0901.0337 [hep-th]].
17. E. M. Lifshitz, *Zh. Eksp. Teor. Fiz.* **29**, 94 (1956) [*Sov. Phys. JETP* **2**, 73, (1956)]; E. M. Lifshitz and L. P. Pitaevskii, *Statistical Physics* (Pergamon Press, Oxford, 1980).
18. M. T. Jaekel and S. Reynaud. *J. De Physique I*, 1(10), 1395–1409, (1991).
19. M. Bordag. *J. Phys.*, A28:755–766, 1995.